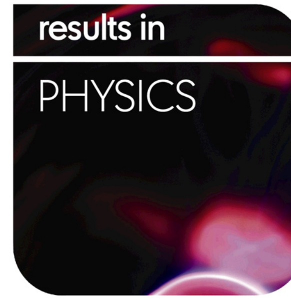

Partial slip and dissipation on MHD radiative ferro-fluid over a non-linear permeable convectively heated stretching sheet

N. Sivakumar, P. Durga Prasad, C.S.K. Raju, S.V.K. Varma, S.A. Shehzad

PII: S2211-3797(17)30649-6
DOI: http://dx.doi.org/10.1016/j.rinp.2017.06.016
Reference: RINP 731

To appear in: *Results in Physics*

Received Date: 18 April 2017
Revised Date: 12 May 2017
Accepted Date: 12 June 2017

Please cite this article as: Sivakumar, N., Durga Prasad, P., Raju, C.S.K., Varma, S.V.K., Shehzad, S.A., Partial slip and dissipation on MHD radiative ferro-fluid over a non-linear permeable convectively heated stretching sheet, *Results in Physics* (2017), doi: http://dx.doi.org/10.1016/j.rinp.2017.06.016

Partial slip and dissipation on MHD radiative ferro-fluid over a non-linear permeable convectively heated stretching sheet

N. Sivakumar[1], P. Durga Prasad[2], C. S. K. Raju[3,4], S.V.K. Varma[2], S.A. Shehzad[5*]

[1]Department of Mathematics, SRM University, Chennai, T.N, India

[2]Department of Mathematics, S.V. University, Tirupati-517502, A.P, India

[3]Department of Mathematics, VIT University, Vellore-632014, T.N, India

[4]Department of Mathematics, Garden City University, Bangalore, K.A, India

[5]Department of Mathematics, COMSATS Institute of Information Technology, Sahiwal 57000, Pakistan

Corresponding author email address: sabirali@ciitsahiwal.edu.pk (S.A. Shehzad)

Abstract:

The simultaneous interaction of viscous dissipative and thermal radiationin MHD two dimensional flows of ferro-liquid over a nonlinear moving surface is analyzed here. The slip on velocity and convective boundary condition on temperature are imposed on stretching surface. We used water as conventional base liquid which have magnetite (Fe_3O_4) and alumina (Al_2O_3) as nanoparticles. The governing mathematical expressions are converted into non-dimensional form via nonlinear type similarity variables. The resulting mathematical model is numerically solved with the help of MATLAB solver bvp4c. The roles of non-dimensional constraints on velocity and temperature are elaborated through plots. The numerical data of skin-friction coefficient and Nusselt number is presented and visualized. The validity of computed results is analyzed through comparative benchmark.

Key words: Ferro fluid; velocity slip condition; convective boundary condition; viscous dissipation; radiation

Nomenclature

u, v : Velocity components in x and y directions

x : Direction along the surface

y : Direction normal to the surface

C_p : Specific heat capacity at constant pressure

f : Dimensionless velocity

m : Non-linear stretching parameter

B : Constant magnetic field

T : Temperature of the fluid

k : Thermal conductivity

T_w : Temperature of wall

T_∞ : Ambient temperature

$\Pr$: Prandtl number

L : Slip length

M : Magnetic field parameter

C_f : Skin friction coefficient

Nu_x : Local Nusselt number

g : Gravitation

Ec : Eckert number

K : Porosity parameter

S : Heat source/sink parameter

n : Power index parameter

C : Constant

u_s : Slip velocity

k_s : Thermal conductivity of nanoparticles

k_f : Thermal conductivity of base fluid

k_{nf} : Thermal conductivity of the nanofluid

Greek Symbols

ϕ : Volume fraction parameter

η : Similarity variable

σ : Electrical conductivity of the fluid

γ : Heat transfer parameter

θ : Dimensionless temperature

λ : Slip parameter

R : Radiation parameter

ρ_{nf} : Density of the nanofluid

μ_{nf} : Dynamic viscosity of nanofluid

υ_{nf} : Kinematic viscosity

μ_{nf} :Effective viscosity

α_{nf} : Thermal diffusivity

χ : Stretching/shrinking parameter

k^{*} :Coefficient of mean absorption

σ^{*} :Constant Stefan-Boltzmann constant

$\left(\rho C_{p}\right)_{f}$: Specific heat parameter of base fluid

$\left(\rho C_{p}\right)_{s}$: Specific heat parameter of nanoparticles

Subscripts

f :Base fluid

s :Solid particles

nf :Nanofluid

∞ :Ambient condition

w : Condition on surface

Superscript

' : Differentiation with respect to η

* : Dimensional properties

1. Introduction

The idea of nanoliquid was initiated by Choi [1] in 1995. He submerged the nanosized particles of aluminum cooper in water and conclude that the involvement of these particles have influential augmentation in heat transport. Nanoliquid is a new variety of fluids. These liquids are very useful in modern technology and industry. The better cooling performance in industrial processes can be achieved through the application of magnetic force. For example, the rate of cooling can be controlled by drawing filaments and continuous strips in electrically conducting nanoliquid [2].The electrically conducting nanoliquids in which the particles like Cobalt Ferrite, Hematite, Magnetite or other compounds having iron are suspended in ordinary liquids are known as ferro-fluids. The dependence on thermal conductivity is due to various factors like shape and size of particle, material of particle, volume fraction, material of base liquid and temperature [3-4].The features of magnetization are explored through ferro-fluids which are non-conducting in nature. In equilibrium condition, the property of magnetization is explored by liquid temperature, intensity of magnetic force, density and various expressions which describe the static magnetization dependence on such quantities. The linear expression of state is the simplest formula. The temperature function is not only described by the coupling of magneto-thermo-mechanical. Here it is also need to involve an equation of magnetic force strength for complete description [5].Based on the importance of ferromagnetic materials; Sheikholeslami et al. [6] considered the ferro-liquid flow in an enclosure under radiation effect. They imposed the constant temperature gradient condition at the wall of enclosure. Here they reported the magneto hydrodynamic (MHD) and ferro-hydrodynamic (FHD) effects simultaneously. In another analysis, Sheikholeslami et al. [7] discussed the features of non-uniform magneto hydrodynamic flow of ferro-liquid with convective heat transport.

The flows arisen due to stretched moving surfaces have multiple physical applications in the branches of chemical engineering and metallurgical processes. Such important applications may include paper production, glass fiber, cooling phenomenon of filaments and strips, plastic production and many more. Crane [8] provided the concept of stretching phenomenon by considering the problem of viscous liquid over moving surface. This outstanding work of Crane has attained the special focus of researchers and engineers and they utilized this concept for the investigation of various fluid flow problems under various circumstances [9-12]. Most of the studies are carried out without slip condition, i.e. it is assumed that fluid particles have zero velocity relative to solid boundary. But literature shows that the characteristics are different in case of micro- and nano-scale fluid flow. Thus, the feature of slip boundary condition was first discussed by Navier [13] in which he states that fluid slip is directly related to shear stress. Das [14] developed a mathematical model by considering the nano-liquid flow over non-linearly moving surface with partially slip condition.

Strek [15] reported the laminar time-dependent ferro-magnetic liquid under the impact of dissipation. Simulations through finite element technique for magneto-ferro-liquid induced by flat surface have been made by Tangthienget al. [16]. Aaiza [17] considered the convective flow of magneto-ferro-liquid past a vertical channel. Puneet [18] studied the magneto hydrodynamic nano-liquid flow under slip and radiation effects. Wahiduzzaman [19] investigated the rotatory flow of nanofluid with dissipation, radiation and magnetic field. Hady et al. [20] elaborated the features of nonlinearly stretched flow of nano-liquid with variable temperature and radiation. Convective heat transport phenomenon of ferro-liquid with magnetohydrodynamic and hydrodynamic effects has been addressed by Sheikholeslami et al. [21]. Li et al. [22] described the features of time-dependent radiative flow of nano-liquid with thermophoresis, magneto hydrodynamics and heat generation impacts. Sheikholeslami and Shehzad [23] reported the importance of radiation in ferro-magnetic fluid flow under the effect of Lorentz force and computed the numerical results. The authors [24-29] are depicted flow over different kind of geometries with various types of flow properties (magnetic field, non-uniform heat source or sink, thermal radiation etc.). The simultaneous effects on heat generation or absorption and thermal radiation in magnetohydrodynamic flow of Maxwell nanofluid towards a stretching sheet explained by Hayat et al. [30]. Recently, the magnetohydrodynamic nanofluid forced convection in a porous lid driven cubic cavity and also the influence of magnetic field on free convection in an open cavity by means of lattice Boltzmann method analyzed by Sheikholeslami [31-32].The influence of Coulomb forces on $Fe_3O_4 - H_2O$ nanofluid thermal improvement was analysed by Sheikholeslami [33]. Sheikholeslami et al. [34] reported the impact of nanofluid two-phase model analysis of induced magnetic field. Sheikholeslami [35-40] investigated about nanofluid thermal behaviours in different configurations.

The main purpose of current study is to investigate the effect of thermal radiation, magnetic field, and viscous dissipation for steady-state ferro-fluid and nanoliquid flow over nonlinearly stretched sheet with convective condition. The governed partial differential relations of flow are reduced into nonlinear coupled ordinary differential systems by using similarity variables. These relations are numerically solved using MATLAB bvp4c.

2. Mathematical Formulation

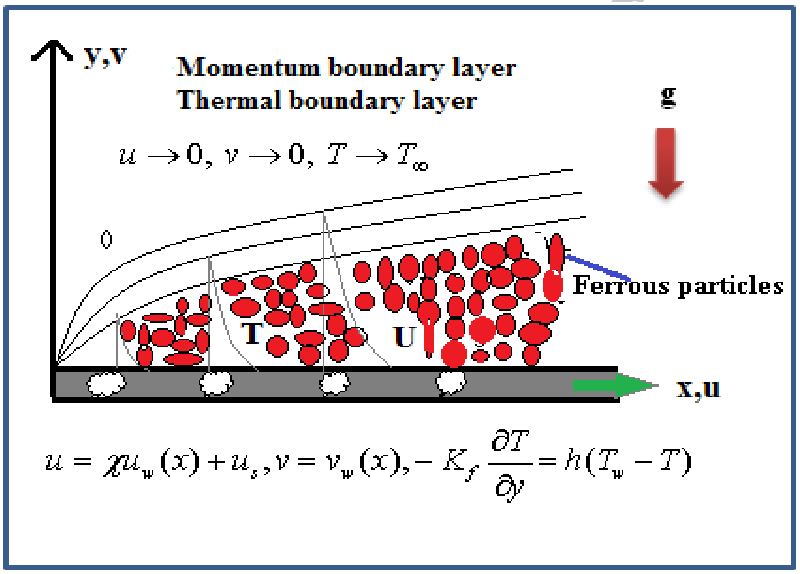

Fig. 1 Physical configuration of the problem

We consider laminar, two-dimensional flow of electrically conducting ferro-liquid over non-linearly stretched sheet with viscous dissipation, radiation and convective condition. Water based nanoliquidis considered which has magnetite and alumina type nanoparticles. A constant magnetic field $B = B_0$ is implemented in the transverse direction to liquid flow. Here the submerged nanoparticles and base liquid are in thermal equilibrium. The sheet is stretched with a velocity $U_w(x) = Cx^n$, where C is a constant, n is a power index and wall mass suction velocity is $v = v_w(x)$ (see Fig. (1)). The pressure gradient and external forces are neglected. Under the above assumptions, the governed expressions (Hady et al. [20]) of momentum and thermal energy are:

$$\frac{\partial u}{\partial x}+\frac{\partial v}{\partial y}=0, \tag{1}$$

$$u\frac{\partial u}{\partial x}+v\frac{\partial u}{\partial y}=\upsilon_{nf}\frac{\partial^2 u}{\partial y^2}-\frac{\sigma B_0^2}{\rho_{nf}}u-\frac{\mu_{nf}}{\rho_{nf}}\frac{\upsilon}{K'}u, \tag{2}$$

$$u\frac{\partial T}{\partial x}+v\frac{\partial T}{\partial y}=\alpha_{nf}\frac{\partial^2 T}{\partial y^2}+\frac{\upsilon_{nf}}{\left(C_p\right)_{nf}}\left(\frac{\partial u}{\partial y}\right)^2-\frac{1}{\left(\rho C_p\right)_{nf}}\frac{\partial q_r}{\partial y}, \tag{3}$$

and the associated conditions to present flow(Parida et al. [41]) are

$$\begin{aligned} &u=\chi u_w(x)+u_s, v=v_w(x), -K_f\frac{\partial T}{\partial y}=h(T_w-T) \quad at \;\; y=0 \\ &u\to 0,\; v\to 0,\; T\to T_\infty \qquad as \;\; y\to\infty \end{aligned} \tag{4}$$

In the present study, we used the subsequent definitions are defined as [7]:

$$\begin{aligned} &\upsilon_{nf}=\frac{\mu_{nf}}{\rho_{nf}}, \rho_{nf}=(1-\phi)\rho_f+\phi\rho_s,\; \mu_{nf}=\frac{\mu_f}{(1-\phi)^{2.5}}, \left(\rho C_p\right)_{nf}=(1-\phi)\left(\rho C_p\right)_f+\phi\left(\rho C_p\right)_s, \\ &\frac{k_{nf}}{k_f}=\frac{\left(k_s+2k_f\right)-2\phi\left(k_f-k_s\right)}{\left(k_s+2k_f\right)+2\phi\left(k_f-k_s\right)} \end{aligned} \tag{5}$$

Table 1: The thermo-physical features of base liquid (water) and nanoparticles (iron oxide and alumina oxide).

Physical Properties	Fluid Phase (Water)	Fe_3O_4	Al_2O_3
$c_p (J/Kg\,K)$	4,179	670	765
$\rho (Kg/m^3)$	997.1	5180	3970
$k (w/mK)$	0.613	9.7	40
$\beta\times 10^{-5}(1/K)$	21	0.5	0.85

The radiative heat flux term by using Roseland approximation is given by [10]:

$$q_r = -\frac{4\sigma^*}{3k^*}\frac{\partial T^4}{\partial y} \tag{6}$$

It is supposed that the differences of temperature in the flow are like that T^4 may be written as a linear combination of temperature [25]:

$$T^4 \cong 4T_\infty^3 T - 3T_\infty^4 \tag{7}$$

Substituting (5) and (6) in (3), we have

$$u\frac{\partial T}{\partial x} + v\frac{\partial T}{\partial y} = \alpha_{nf}\frac{\partial^2 T}{\partial y^2} + \frac{16\sigma T_\infty^3}{3\left(\rho C_p\right)_{nf} k^*}\frac{\partial^2 T}{\partial y^2} + \frac{\upsilon_{nf}}{\left(C_p\right)_{nf}}\left(\frac{\partial u}{\partial y}\right)^2 \tag{8}$$

3. Method of Solution

Now, we introduce the following similarity transforms and dimensionless quantities as

$$\eta = y\sqrt{\frac{C(n+1)}{2\upsilon_f}}x^{\frac{n-1}{2}},\ u = Cx^n f'(\eta), v = -y\sqrt{\frac{C(n+1)\upsilon_f}{2}}x^{\frac{n-1}{2}}\left(f(\eta) + \frac{n-1}{n+1}\eta f'(\eta)\right),$$
$$\theta(\eta) = \frac{T - T_\infty}{T_w - T_\infty}, \tag{9}$$

The implementation of above variables leads to the following expressions

$$f''' + (1-\phi)^{2.5}\left(1-\phi+\phi\frac{\rho_s}{\rho_f}\right)\left(ff'' - \frac{2n}{n+1}f'^2\right) - \left(M(1-\phi)^{2.5} + K\right)f' = 0 \tag{10}$$

$$\left(\frac{k_{nf}}{k_f} + \frac{4R}{3}\right)\theta'' + \frac{\Pr Ec}{(1-\phi)^{2.5}}\left(f''\right)^2 + \Pr\left[(1-\phi) + \phi\frac{\left(\rho C_p\right)_s}{\left(\rho C_p\right)_f}\right]\left(f\theta' - \frac{2m}{n+1}f'\theta\right) = 0 \tag{11}$$

$$f = S,\ f' = \chi + \lambda f'',\ \theta'(0) = -\gamma\left[1 - \theta(0)\right]$$
$$f'(\infty) = 0,\ \theta(\infty) = 0 \tag{12}$$

In above expressions,

$$M=\frac{2\sigma B_0^2 x}{\rho_f U_w(n+1)},\ K=\frac{2\upsilon_f x}{K' U_w(n+1)},\ Ec=\frac{U_w{}^2}{\left(c_p\right)_f\left(T_w-T_\infty\right)},\ R=\frac{4\sigma^* T_\infty^3}{kk^*}\ \Pr=\frac{\left(\mu c_p\right)_f}{k_f}.$$

The interested physical quantities are the coefficient of skin-friction C_{fx} and Nusselt number Nu_x are

$$C_{fx}=\frac{2\mu_{nf}}{\rho_f\left(u_w\left(x\right)\right)^2}\left(\frac{\partial u}{\partial y}\right)_{y=0} \tag{13}$$

$$Nu_x=\frac{-k_{nf}x}{k_f(T_w-T_\infty)}\left(\frac{\partial T}{\partial y}\right)_{y=0} \tag{14}$$

The above equations in non-dimensional form can be described as

$$\sqrt{\frac{C}{2\upsilon_f}}C_f=\frac{\sqrt{n+1}}{\left(1-\phi\right)^{2.5}}x^{-\frac{n+1}{2}}f''\left(0\right) \tag{15}$$

$$\sqrt{\frac{2\upsilon_f}{C}}Nu_x=-\frac{k_{nf}\sqrt{n+1}}{k_f}x^{\frac{n+1}{2}}\theta'\left(0\right) \tag{16}$$

4. Results and Discussion

The derived nonlinear ordinary differential expressions (10)-(12) are tackled numerically by using bvp4c with MATLAB package. The numerically computed results are visualized for various values of flow parameters on liquid velocity and temperature to describe the features of these parameters. Figs. 2-13 are prepared for this task. The factor of skin-friction and Nusselt number are computed and shown in tabular form. The role of volume fraction of ferro-liquid ϕ on flow and heat transport is examined in range $0 \le \phi \le 0.2$, where $\phi=0$ is the case of pure liquid. The thermo physical features of base liquid, the nano and ferrofluids are listed in Table1.

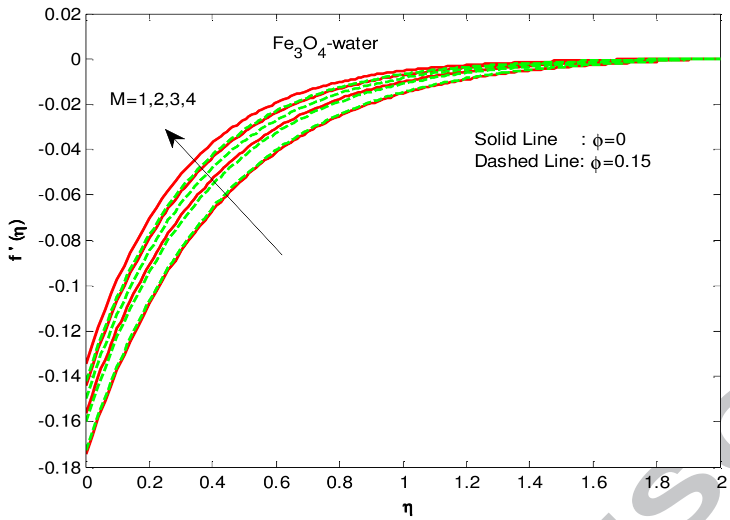

Fig. 2: Curves of velocity for different M with fixed value $\chi = 1$,

$R = 0.1, S = 2, \gamma = 0.1, n = 10, m = 20, \lambda = 2, \Pr = 6.2, K = 0.1, Ec = 0.1$

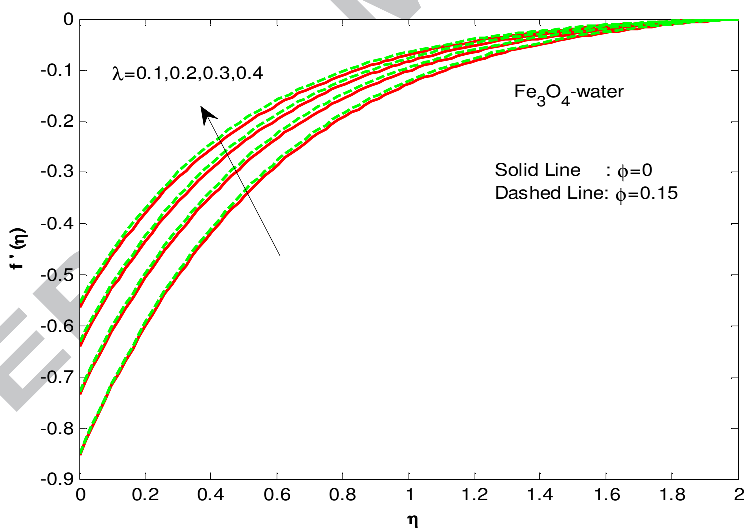

Fig. 3: Curves of velocity for different λ with fixed value $\chi = 1$,

$S = 2, M = 0.5, R = 0.1, \gamma = 0.1, n = 10, m = 20, \lambda = 2, \Pr = 6.2, K = 0.1, Ec = 0.1$.

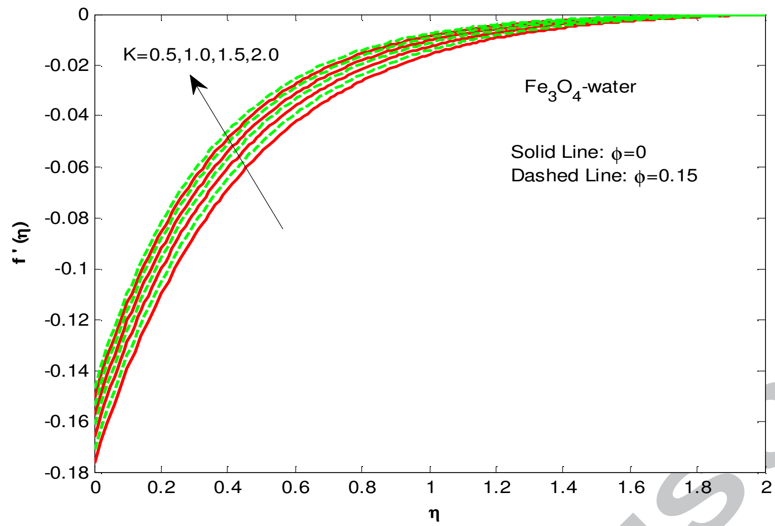

Fig. 4: Curves of velocity for different K with fixed value $\chi = 1$,

$S = 2, M = 0.5, R = 0.1, \gamma = 0.1, n = 10, m = 20, \lambda = 2, \Pr = 6.2, Ec = 0.1$.

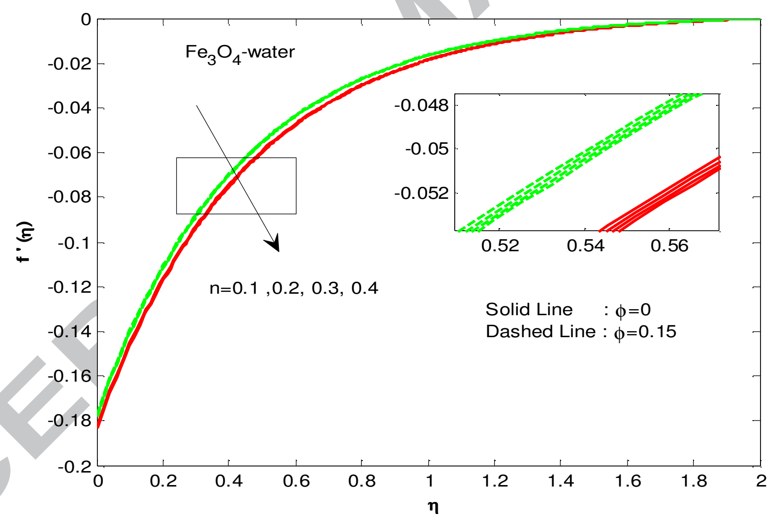

Fig. 5: Curves of velocity for different n with fixed value $\chi = 1$,

$S = 0.5, M = 0.2, R = 0.1, \gamma = 5, m = 2, \lambda = 0.5, \Pr = 6.2, Ec = 0.5, K = 5$.

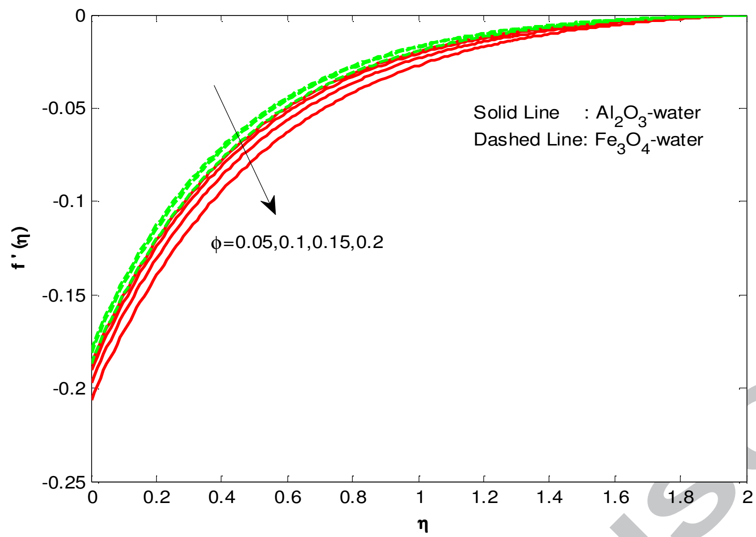

Fig. 6: Curves of velocity for different ϕ with fixed value $\chi = 1$

$S = 2, M = 0.5, R = 0.1, \gamma = 0.1, m = 20, \lambda = 2, \Pr = 6.2, Ec = 0.1, K = 0.1$.

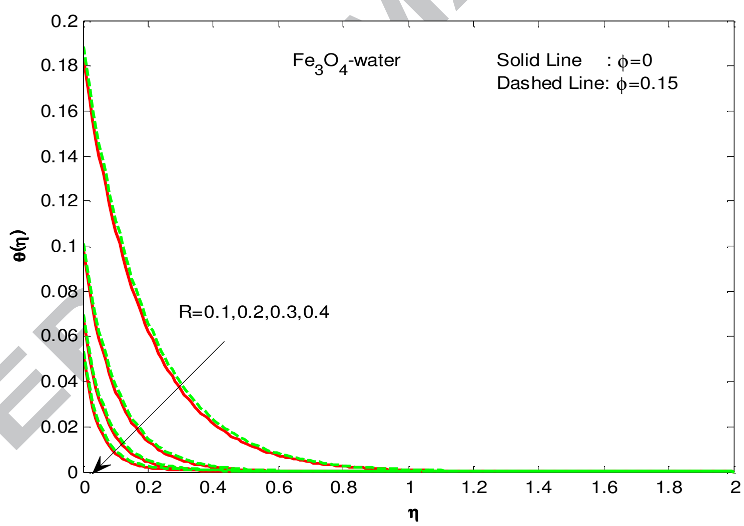

Fig. 7: Curves of velocity for different R with fixed value $\chi = 1$,

$S = 2, M = 0.5, \gamma = 0.1, n = 10, m = 20, \lambda = 2, \Pr = 6.2, K = 0.1, Ec = 0.1$.

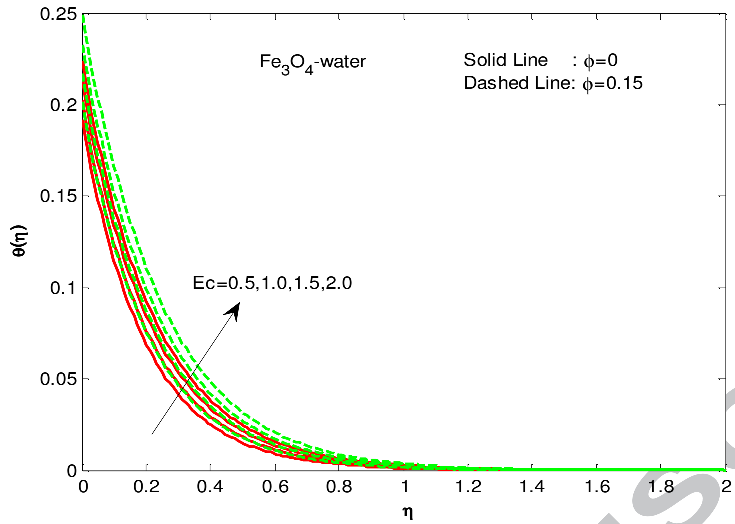

Fig. 8: Curves of temperature for different Ec with fixed value $\chi = 1$,

$S = 2, M = 0.5, R = 0.1, \gamma = 0.1, n = 10, m = 20, \lambda = 2, \Pr = 6.2, Ec = 0.1, K = 0.1$.

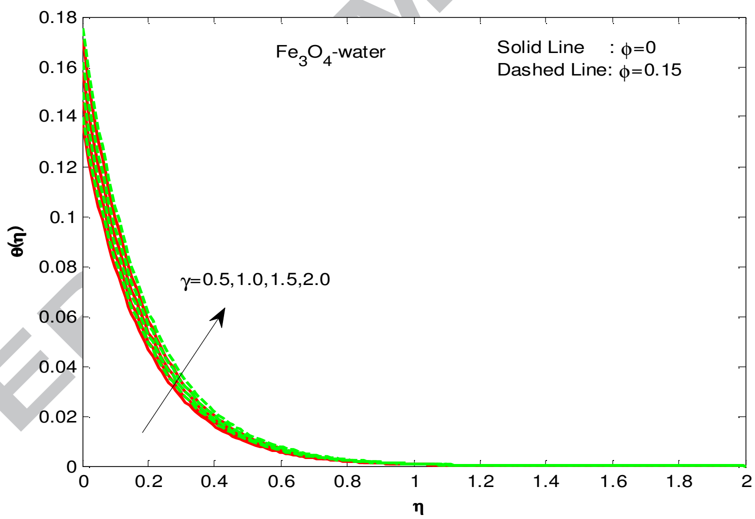

Fig. 9: Curves of temperature for different γ with fixed value $\chi = 1$,

$S = 2, M = 0.5, R = 0.1, \gamma = 0.1, n = 10, m = 20, \lambda = 2, \Pr = 6.2, Ec = 0.1, K = 0.1$.

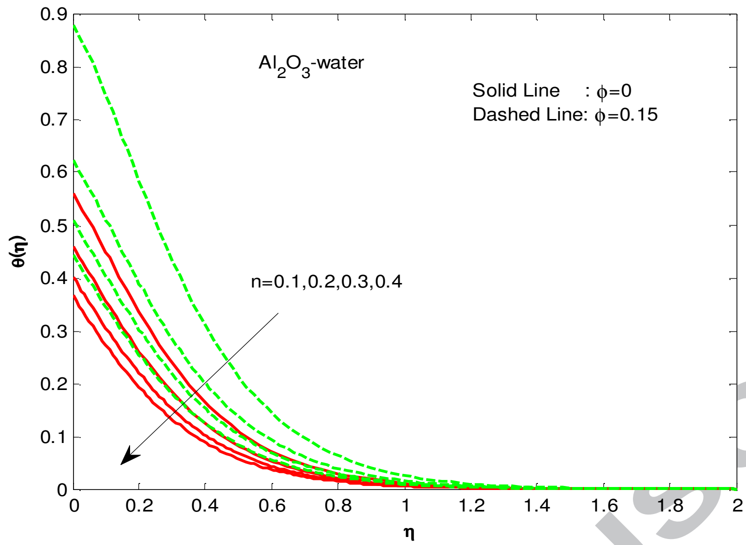

Fig. 10: Curves of temperature for different n with fixed value $\chi = 1$,

$S = 2, M = 0.5, R = 0.1, \gamma = 0.1, m = 20, \lambda = 2, \Pr = 6.2, Ec = 0.1, K = 0.1$.

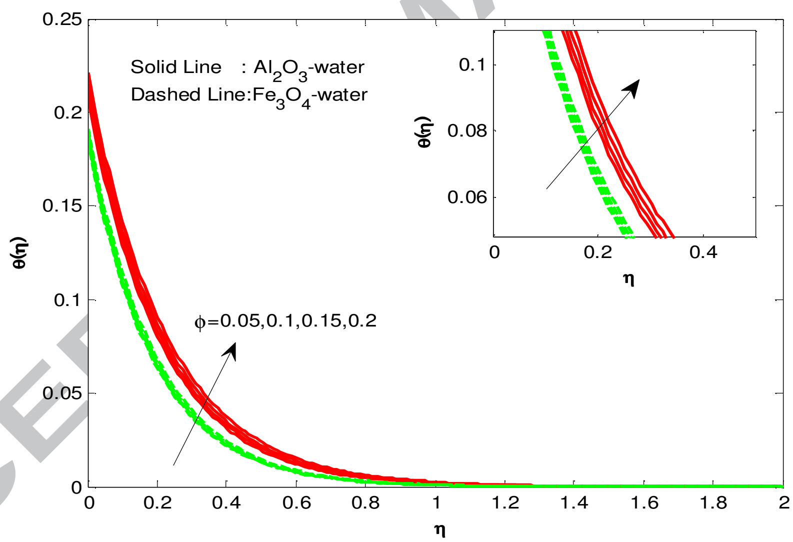

Fig. 11: Curves of temperature for different ϕ with fixed value $\chi = 1$,

$S = 2, M = 0.5, R = 0.1, \gamma = 0.1, n = 10, m = 20, \lambda = 2, \Pr = 6.2, Ec = 0.1, K = 0.1$.

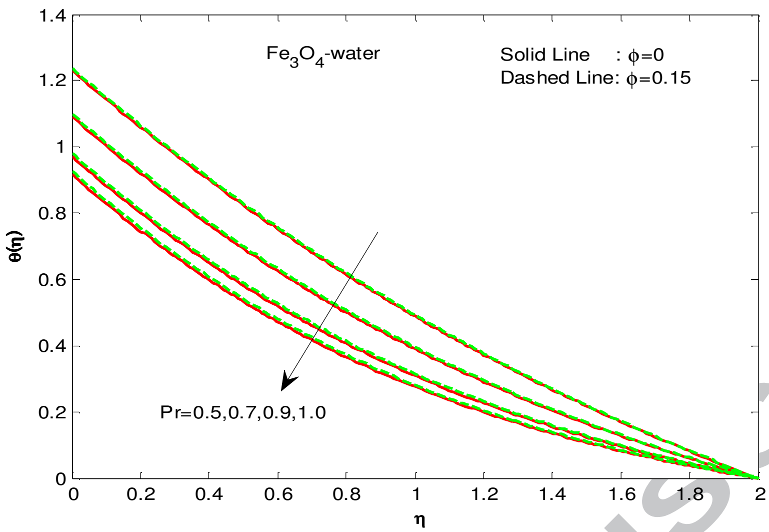

Fig. 12: Curves of temperature for different Pr with fixed value $\chi = 1$,

$S = 2, M = 0.5, R = 0.1, \gamma = 0.1, n = 10, m = 20, \lambda = 2, \Pr = 6.2, Ec = 0.1, K = 0.1$.

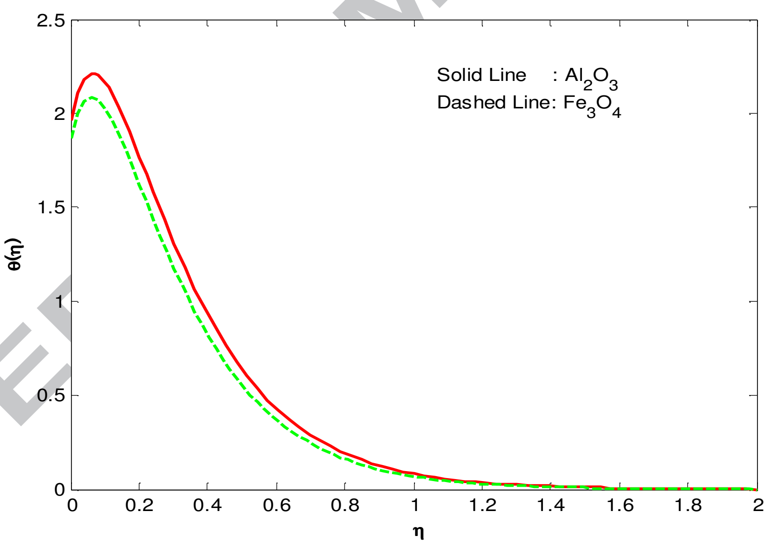

Fig. 13: Comparative results of ferrofluid (Fe_3O_4) velocity with nanofluid (Al_2O_3) velocity when $\phi = 0.5$.

Fig. 2 shows the variation of velocity profiles of ferro-fluid for various *M*. The liquid velocity adjacent to wall and inside boundary layer is improved with an enhancement in magnetic parameter. The addition of last two terms in momentum expression is positive due to which liquid motion in region of boundary layer enhances. Generally, the magnetic force pushes the electrically conducting liquid due to which magnetic field has influential role to manipulate the liquid in the system of micro scale.

Fig. 3 displays the curves of velocity for various values of slip parameter for the case of ferro-fluid. The velocity of ferro-liquid boosts up for larger λ. The motion at liquid-solid interface enhances due to the increasing velocity slip factor. The velocity of stretched surface and adjacent velocity of solid surface match in the case of no-slip assumption i.e. $f' = \chi = 1$.The changes in the velocity for various permeability parameter K are reported in Fig. 4. Here we noted that K is the inverse of Darcian drag force in porous space. Thus, a larger value of K signifies rather low resistance by the porous medium to cause more ease for fluid transversal in porous medium. Hence, for larger values of K, the thickness of momentum boundary layer increases. The effect of stretching parameter n on the velocity and temperature distribution is elaborated in Figs. 5 and 10. The flow is observed to be strongly decelerated with higher n. The effect of increasing stretching rate is to destroy velocity and temperature development.

Figs. 6 and 11 described the enhancement in volume fraction ϕ leads a retardation in velocity but the temperature increases. We also noticed that the temperature of Fe_3O_4 -water ferrofluid is lesser as the temperature of Al_2O_3 -water nanoliquid. The enhancement in volume fraction is responsible for the larger profiles of temperature. Generally, the thermal conductivity is stronger for larger volume fraction factor. The influence of radiative parameter R on temperature of ferro-liquid is shown in Fig. 7. The temperature of ferro-liquid is retarded for the higher radiative parameter. A thinner thickness of boundary layer is appeared with the use of larger radiative parameter. Fig. 8 displays the variation of on temperature for various Eckert number in the cases of water based magnetite ferrofluid and Al_2O_3 nanofluid. The liquid temperature is larger for magnetite and non-magnetite Eckert number. For $Ec = 0$, the term of viscous dissipation can be ignored in the expression of energy. Hence the temperature is smaller when Eckert number goes to zero. The energy is enhanced with an increase in Ec due to which liquid temperature is boost up.

It is observed from Fig. 9 that temperature corresponding to larger convective heat transfer parameter γ is risen. Physically, a decrease in hot fluid side convection is produced with an increase in convective heat transfer and resultantly the surface temperature increases. The variation of temperature profiles against different Prandtl number ($\Pr$) is presented in Fig. 12 for both ferrofluid and nanofluid. Here we revealed that the temperature retards for larger values of $\Pr$. The thermal diffusivity is reduced with the enhancing values of Pr due to that thinner thickness of layer is achieved. The comparison of velocity profiles for nanofluid and ferrofluid is shown in Fig. 13. From this figure it was found that the velocity of Al_2O_3 nanofluid was greater than the velocity of the ferrofluid. This is due to fact that conductivity and viscosity of ferro-liquids greater than Al_2O_3 nanoliquid.

To verify the accuracy of present computations, we considered the solutions of Cortell [24] in a limiting way. We compared the values of Nusselt number with [24] for pure liquid $(\phi = 0)$. Table 2 is computed for this analysis. Our present computations have good match with [24] in limiting sense (see Table 2).The numerical values of convective heat transport parameter γ, radiative factor R and Eckert number Ec on coefficients of skin-friction and heat transport for both nanofluid and ferrofluid is presented in Table 3.An enhancement in γ and Ec reduces the Nusselt number while it enhances for higher R .Moreover, the coefficient of skin-friction decrease due to an increase in γ .

Table 2: Comparison of the values of $-\theta'(0)$ with $\phi = 0$, $R = 0$, $\lambda = 0$, $\chi = 1$, $S = 0$ and $\gamma \to \infty$.

$-\theta'(0)$					
Ec	n	$\Pr = 1$		$\Pr = 5$	
		Cortell [24]	Present results	Cortell [24]	Present results
0.0	0.75	1.252672	1.253490	3.124975	3.123644
	1.5	1.439393	1.439370	3.567737	3.566540
	7	1.699298	1.698746	4.185373	4.184382
	10	1.728934	1.728344	4.255972	4.254931
0.1	0.75	1.219985	1.220306	3.016983	3.013652
	1.5	1.405078	1.404797	3.455721	3.453163
	7	1.662506	1.661711	4.065722	4.063753
	10	1.691822	1.690995	4.135296	4.133331

Table 3: Numerical values of skin friction coefficient $f^{''}(0)$ and Nusselt number $-\theta^{'}(0)$ for both nanofluid and ferrofluid with $S = 2, \Pr = 6.2, \chi = 1, \lambda = 2, M = 0.5, K = 0.1$

γ	R	Ec	Al_2O_3 $-\theta^{'}(0)$	Fe_3O_4 $-\theta^{'}(0)$	Al_2O_3 $f^{''}(0)$	Fe_3O_4 $f^{''}(0)$
0.2	0.5	0.2	0.990229	0.990699	0.406550	0.409797
0.4	0.5	0.2	0.980621	0.981548	0.404857	0.407631
0.6	0.5	0.2	0.971172	0.972541	0.397239	0.406921
0.5	**0.1**	0.2	0.899297	0.911060	0.401754	0.409618
0.5	**0.2**	0.2	0.945867	0.949865	0.401754	0.409618
0.5	**0.3**	0.2	0.962363	0.964566	0.401754	0.409618
0.5	0.5	**0.3**	0.944217	0.975509	0.401754	0.409618
0.5	0.5	**0.4**	0.942568	0.973991	0.401754	0.409618
0.5	0.5	**0.5**	0.940918	0.972473	0.401754	0.409618

5. Conclusions

The aim of present analysis is to obtain the solutions of nonlinearly stretched flows of ferro-liquid. The involvement of radiative heat flux in energy expression is described by the approximation of Roseland. The effect of the pertinent constraints on liquid velocity and temperature is visualized graphically. The most important concluding remarks can be reported as follows:

- The velocity with the increasing slip parameter λ is enhanced. Physically, this happens due to fact that the velocity slip enhances the velocity at the fluid-solid interface.
- The dimensionless temperature increases with increasing Eckert number Ec while it decreases with increasing thermal radiation parameter R.
- The larger convective parameter γ leads to higher temperature and thicker thickness of boundary layer associated to temperature.
- Increase in the value of γ, and Ec results in decrease of the rate of heat transport.

Acknowledgement:

The authors would like to thank the anonymous reviewers for their valuable comments and suggestions to improve the quality of the paper.

References:

[1]. S.U.S Choi, Enhancing Thermal Conductivity of Fluids with nanoparticles, Developments and Application of Non-Newtonian Flows, D.A. Siginer and H.P. Wang, eds, FED-Vol. 231/MD-ASME, New York,66(2005)99-105.

[2]. A.B. Rosmila, R. Kandasamy, I. Muhaimin, Lie symmetry group transformation for MHD natural convection flow of nanofluid over a linearly stretching sheet in the presence of thermal stratification, Appl. Math. Mech. 33 (2012) 593–604.

[3]. C.S. K. Raju, N. Sandeep, Unsteady Casson nanofluid flow over a rotating cone in a rotating frame filled with ferrous nanoparticles: A numerical study, J. Magnet. Magnet. Mater. 421 (2017) 216-224.

[4]. S. Ozernic, S. Kakac, A.G. Yazicioglu, Enhanced thermal conductivity of nanofluids: A state of the art review, Micro fluid. Nanofluid. 8 (2012) 145–170.

[5]. H. Matsuki, K. Yamasawa, K. Murakami, Experimental considerations on a new automatic cooling device using temperature sensitive magnetic fluid. IEEE Transac. Magnet. 13(1997)1143-1145.

[6]. M. Sheikholeslami, D.D. Ganji, M.M. Rashidi, Ferrofluid flow and heat transfer in a semi annulus enclosure in the presence of magnetic source considering thermal radiation, J. Taiwan Inst. Chem. Eng. 47 (2015) 6-17.

[7]. M. Sheikholeslami, M.M. Rashidi, D.D. Ganji, Effect of non-uniform magnetic field on forced convection heat transfer of Fe_3O_4-water nanofluid, Comput. Methods Appl. Mech. Eng. 294 (2015) 299-312.

[8]. L.J. Crane, Flow past a stretching plate, Z. Angew. Math. Phys. 21 (1970) 645–647.

[9]. V.M. Soundalgekar, T.V. Ramanamurthy, Heat transfer past a continuous moving plate with variable temperature, Warme Stoffubertrag14 (1980) 91–93.

[10]. L. Zheng, C. Zhang, X. Zhang, J. Zhang, Flow and radiation heat transfer of a nanofluid over a stretching sheet with velocity slip and temperature jump in porous medium, J. Frank. Inst. 350 5 (2013) 990-1007.

[11]. Y. Lin, L. Zheng, X. Zhang, Radiation effects on Marangoni convection flow and heat transfer in pseudo-plastic non-Newtonian nanofluids with variable thermal conductivity, Int. J. Heat Mass Transfer 77 (2014) 708-716.

[12]. T. Hayat, M. Waqas, M.I. Khan, A. Alsaedi, S.A. Shehzad, Magnetohydrodynamic flow of Burgers fluid with heat source and power law heat flux, Chin. J. Phys. 55 (2017) 318-330.

[13]. C.L.M.H. Navier, Memoire sur leslois du movement des fluids, Mem. Acad. R Sci. Inst. France 6 (1823) 389–440.

[14]. K. Das, Nanofluid flow over a non-linear permeable stretching sheet with partial slip, J. Egypt. Math. Soc. 23 (2015) 451–456.

[15]. T. Strek, Ferrofluid channel flow under the influence of magnetic dipole. Int. J. Applied Mech. Eng. 10 (2005)103-109.

[16]. C. Tangthieng, B.A. Finlayson, J. Maulbetsch, T. Cader, Heat transfer enhancement in ferrofluids subjected to steady magnetic fields, J. Magnet. Magnet. Mater.201 (1999) 252–255.

[17]. G. Aaiza, I. Khan. S. Shafie, A. Khalid. A. Khan, Heat transfer in MHD mixed convection flow of a ferrofluid along a vertical channel, Plos One 10(2015)1-14.

[18]. R. Puneet, D. Ruchika, K. Lokendra, Radiative nanofluid flow and heat transfer over a non-linear permeable sheet with slip conditions and variable magnetic field: Dual solutions.Ain Shams Engineering Journal (2015) doi.org/10.1016/j.asej.2015.08.016.

[19]. M. Wahiduzzaman, M. Khan, P. Biswas, I. Karim, M.J. Uddin, Viscous dissipation and radiation effects on MHD boundary layer flow of a nanofluid past a rotating stretching sheet, Appl. Math. 6(2015)547-567.

[20]. F.M. Hady, F.S. Ibrahim., S.M. Abdel-Gaied, M.R. Eid, Radiation effect on viscous flow of a nanofluid and heat transfer over a nonlinearly stretching sheet, Nanoscale Research Lett. **7** (2012) 1-13.

[21]. M. Sheikholeslami, D.D. Ganji, Ferrohydrodynamic and magnetohydrodynamic effects on ferrofluid flow and convective heat transfer, Energy 75 (2014) 400-410.

[22]. J. Li, L. Liu, L. Zheng, B. Bin-Mohsin, Unsteady MHD flow and radiation heat transfer of nanofluid in a finite thin film with heat generation and thermophoresis, J. Taiwan Inst. Chem. Eng. 67 (2016) 226-234.

[23]. M. Sheikholeslami, S.A. Shehzad, Thermal radiation of ferrofluid in existence of Lorentz forces considering variable viscosity, Int. J. Heat Mass Transfer 109 (2017) 82-92.

[24]. R. Cortell, Viscous flow and heat transfer over a nonlinearly stretching sheet, Appl. Math. Comput. 184(2007)864-873.

[25]. K. Hsiao, Energy conversion conjugate conduction-convection and radiation over non-linearly extrusion stretching sheet with physical multimedia effects, Energy 59 (2013) 494-502.

[26]. K. Hsiao, Combined electrical MHD heat transfer thermal extrusion system using Maxwell fluid with radiative and viscous dissipation effects, Appl. Thermal Eng. 112 (2017) 1281-1288.

[27]. C.S.K. Raju, S.M. Ibrahim, S. Anuradha, P. Priyadharshini, Bio-convection on the nonlinear radiative flow of a Carreau fluid over a moving wedge with suction or injection, Europ. Phys. J. Plus 131 (2016) 409.

[28]. C.S. K. Raju, N Sandeep, ME Ali, Effect of temperature dependent viscosity on MHD radiative nanofluid flow caused by heated/cooled cone, J. Comput. Theoret. Nanosci. 14 (2017) 821-828.

[29]. T. Muhammad, A. Alsaedi, S.A. Shehzad, T. Hayat, A revised model for Darcy-Forchheimer flow of Maxwell nanofluid subject to convective boundary condition, Chin. J. Phys. http://dx.doi.org/10.1016/j.cjph.2017.03.006.

[30]. T. Hayat , S. Qayyum, S.A. Shehzad, A. Alsaedi, Simultaneous effects of heat generation/absorption and thermal radiation in magnetohydrodynamics (MHD) flow of Maxwell nanofluid towards a stretched surface, Results Phys. 7 (2017) 562-573.

[31]. M. Sheikholeslami, Magnetohydrodynamic nanofluid forced convection in a porous lid driven cubic cavity using Lattice Boltzmann method, J. Mol. Liq. 231 (2017) 555-56.

[32]. M. Sheikholeslami, Influence of magnetic field on nanofluid free convection in an open porous cavity by means of Lattice Boltzmann method, J. Mol. Liq. 234 (2017)

[33]. M. Sheikholeslami, Influence of Coulomb forces on Fe_3O_4-H_2O nanofluid thermal improvement, Int. J. Hydrogen Energy 42 (2017) 821-829.

[34]. M. Sheikholeslami, H.B. Rokni, Nanofluid two phase model analysis in existence of induced magnetic field, Int. J. Heat Mass Transf. 107 (2017) 288–299.

[35]. M. Sheikholeslami, CuO-water nanofluid free convection in a porous cavity considering Darcy law, Europ. Phys. J. Plus 132 (2017) 55.

[36]. M. Sheikholeslami, Magnetic field influence on nanofluid thermal radiation in a cavity with tilted elliptic inner cylinder, J. Mol. Liq. 229 (2017) 137-147.

[37]. M. Sheikholeslami, Numerical simulation of magnetic nanofluid natural convection in porous media, Phys. Lett. A 381 (2017) 494-503.

[38]. M. Sheikholeslami, Magnetic source impact on nanofluid heat transfer using CVFEM, Neural Comput. Appl. (2016) DOI 10.1007/s00521-016-2740-7.

[39]. M. Sheikholeslami, Influence of Lorentz forces on nanofluid flow in a porous cylinder considering Darcy model, J. Mol. Liq. 225 (2017) 903-912.

[40]. M. Sheikholeslami, S.A. Shehzad, Magnetohydrodynamic nanofluid convection in a porous enclosure considering heat flux boundary condition, Int. J. Heat Mass Transf. 106 (2017) 1261-1269.

[41]. S.K. Parida, S. Panda, B.R. Rout, MHD boundary layer slip flow and radiative nonlinear heat transfer over a flat plate with variable fluid properties and thermophoresis, Alex. Eng. J. 54 (2015) 941-953.

Highlights

- The simultaneous interaction of viscous dissipative and thermal radiation is incorporated.
- MHD two dimensional flow of ferro-liquid is modeled.
- We used water as conventional base liquid which have magnetite (Fe_3O_4) and alumina (Al_2O_3) as nanoparticles.
- The validity of computed results is analyzed through comparative benchmark.